PHYSICAL REVIEW E **87**, 020102(R) (2013)

Scale-invariant growth processes in expanding space

Adnan Ali,[1] Robin C. Ball,[1,2] Stefan Grosskinsky,[1,3] and Ellák Somfai[1,2,*]
[1]*Centre for Complexity Science, University of Warwick, Coventry CV4 7AL, United Kingdom*
[2]*Department of Physics, University of Warwick, Coventry CV4 7AL, United Kingdom*
[3]*Mathematics Institute, University of Warwick, Coventry CV4 7AL, United Kingdom*
(Received 13 July 2012; published 7 February 2013)

Many growth processes lead to intriguing stochastic patterns and complex fractal structures which exhibit local scale invariance properties. Such structures can often be described effectively by space-time trajectories of interacting particles, and their large scale behavior depends on the overall growth geometry. We establish an exact relation between statistical properties of structures in uniformly expanding and fixed geometries, which preserves the local scale invariance and is independent of other properties such as the dimensionality. This relation generalizes standard conformal transformations as the natural symmetry of self-affine growth processes. We illustrate our main result numerically for various structures of coalescing Lévy flights and fractional Brownian motions, including also branching and finite particle sizes. One of the main benefits of this approach is a full, explicit description of the asymptotic statistics in expanding domains, which are often nontrivial and random due to amplification of initial fluctuations.

DOI: 10.1103/PhysRevE.87.020102 PACS number(s): 05.40.−a, 89.75.Da, 61.43.Hv, 87.18.Hf

Scale-invariant structures resulting from fractal growth processes are abundant across nature [1,2]. Examples include diffusion-limited aggregation [3], river basins [4], and self-affine domain boundaries forming behind growing fronts for spatial competition models [5,6]. While first results appeared already 30 years ago, the field continues to be of interest [7] with recent applications in microbial growth [8,9]. In many cases these structures can be modeled as trajectories of locally interacting particles—a picture that we adopt in this Rapid Communication. The overall geometry has a strong impact on growth processes. A dramatic example is viscous fingering, where in constant width channel geometry a stable Saffman-Taylor finger of fixed shape propagates [10], while in radial geometry a continuously tip splitting branched structure emerges [11,12]. In biological growth spatial range expansion is often coupled to drift and competition in the genetic pool [13], and is recognized to have major influence on the gene pool of natural populations [14].

In this Rapid Communication we show how the effect of the overall geometry in many directed growth processes can be captured elegantly in terms of a time-dependent metric. We view growing domain boundaries as space-time trajectories of particles moving on the growth front, which is expanding in many interesting cases. A natural example within the scope of this Rapid Communication is isoradial growth in two dimensions, such as domain boundaries of competing microbial species in a petri dish [8]. While cosmology is an obvious example, there has been recent interest in nonconstant metric also in thin sheets [15–17]. Our results are applicable to the formation of stochastic patterns and structures in a very general setting, including diffusion processes with time-dependent diffusion rate (i.e., temperature) [18–21], in cosmologically expanding space [22], or on a biologically growing substrate.

In particular, we consider self-affine space-time trajectories of particles under spatially homogeneous but time-dependent metric, and map those into more easily tractable systems with constant metric. The mapping depends only on the local scale invariance exponent of the trajectories, and works directly for local interactions which do not involve a length scale, such as annihilation or coagulation of point particles. Branching, exclusion and reflection of finite size particles can also be treated after mapping the interaction length scales appropriately. This provides a natural extension of conformal maps to generalized self-affine growth processes, and we show how this leads to an exact description of the nontrivial asymptotic statistics of growth structures in expanding domains, which is one particularly striking consequence of this approach.

To describe our results in the most illustrative setting, we consider the growth of self-affine structures (e.g., domain boundaries) in isoradial geometry in two dimensions. These structures consist of directed "arms," which can be interpreted as locally scale-invariant space-time trajectories of point particles moving in an expanding one-dimensional space with periodic boundary conditions.

Consider an isotropic radial structure growing from an initial disk with radius r_0, shown in Fig. 1(a) for an example of radial coalescing Brownian motions, where also the following notation is illustrated. We describe each arm by the displacement along the perimeter of the growing circle

$$Y_r \in [0,2\pi r) \quad \text{with} \quad r \geqslant r_0 \tag{1}$$

as a function of the radial distance r; directed radial growth means that this is possible. In the increment

$$dY_r = Y_r\, dr/r + d\tilde{Y}_r \tag{2}$$

the first term is due to the stretching of space, and the second corresponds to the inherent fluctuations encoding the local scale invariance of the arms. Instead of radial coordinates (Y,r), the arms can also be represented in modified polar coordinates (X,h): The polar angle is multiplied by r_0 and denoted by X_h, which is in a fixed periodic domain,

$$X_h \in [0,L) \quad \text{with} \quad h \geqslant 0, \tag{3}$$

*Present address: Wigner RCP SZFI, P.O. Box 49, H-1525 Budapest, Hungary.

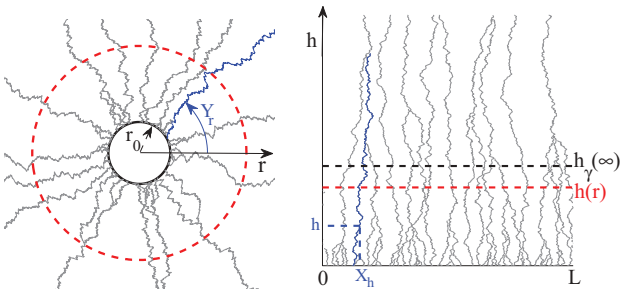

FIG. 1. (Color online) Expanding radial growth structure and the same structure on a fixed domain with periodic boundary conditions, illustrated for the case of coalescing random walks ($\gamma = 1/2$). The displacements Y_r [Eq. (1)] and X_h [Eq. (3)] are shown as blue (dark gray) curves. The distribution of the rescaled radial structure at radius r is identical to the distribution of the fixed domain structure at height $h(r)$ as given by Eq. (8), indicated by dashed red (gray) lines. This mapping (plotted in Fig. 2) has a finite limit $h_\gamma(\infty)$ for $\gamma < 1$, indicated by a dashed black line. Parameters are $L = 100$ with $r_0 = L/2\pi$, unit diffusion coefficient, and initially 100 arms.

and the relation between r and h will be determined shortly. The choice $L = 2\pi r_0$ enables matching the initial conditions between $X_{h=0}$ and $Y_{r=r_0}$. This implies

$$X_h = \frac{r_0}{r} Y_r, \tag{4}$$

which using Eq. (2) yields for the increments

$$dX_h = \frac{r_0}{r} d\tilde{Y}_r. \tag{5}$$

We impose that the mapping between expanding and fixed geometry preserves the relevant local structure of the object (analogously to conformal invariance), which in our case is given by local scale invariance of the arms

$$dX_h \sim (dh)^\gamma \quad \text{and} \quad d\tilde{Y}_r \sim (dr)^\gamma, \tag{6}$$

with $\gamma > 0$. For example, diffusive fluctuations correspond to $\gamma = 1/2$ (see Ref. [23] for related results), and for ballistic displacements of the arms $\gamma = 1$. Other values are related to sub- or superdiffusive behavior, such as $\gamma = 2/3$ for domain boundaries driven by a surface in the Kardar-Parisi-Zhang (KPZ) universality class [6,24,25].

This leads to a relationship between $h \geqslant 0$ and $r \geqslant r_0$ via

$$\frac{dh}{dr} = \left(\frac{dX_h}{d\tilde{Y}_r}\right)^{1/\gamma} = \left(\frac{r_0}{r}\right)^{1/\gamma}, \tag{7}$$

where multiplicative prefactors, which are equal in Eq. (6) although not indicated, drop out. Integrating yields

$$h(r) = \begin{cases} r_0 \frac{\gamma}{1-\gamma}[1 - (r_0/r)^{\frac{1-\gamma}{\gamma}}], & \gamma \neq 1, \\ r_0 \ln(r/r_0), & \gamma = 1, \end{cases} \tag{8}$$

for all $r \geqslant r_0$. For a single arm the matching initial condition $Y_{r_0} = X_0$ leads to identical distributions $\frac{r_0}{r} Y_r \overset{\text{dist.}}{=} X_{h(r)}$ for all $r \geqslant r_0$. Our main result is now that the same holds for the entire growth structures, which are characterized as collections of arms $\{Y_r\}$ and $\{X_h\}$, with the independent variables linked through $h = h(r)$:

$$\left\{\frac{r_0}{r} Y_r\right\} \overset{\text{dist.}}{=} \{X_{h(r)}\} \quad \text{for all} \quad r \geqslant r_0, \tag{9}$$

provided that the arms interact only locally. Examples of such interactions include coagulation or annihilation, and we discuss how this can be generalized in more detail below. Figure 1 illustrates this correspondence for coalescing Brownian trajectories.

Properties of the mapping. To leading order $h(r) \approx r - r_0$ for r close to r_0, since locally the fixed domain and the radial models are equivalent. The effect of the different geometries enters in the nonlinear behavior of $h(r)$ for larger values of r, in particular, for $0 < \gamma < 1$ we have

$$h_\gamma(\infty) = \lim_{r\to\infty} h(r) = \frac{\gamma}{1-\gamma} r_0 < \infty. \tag{10}$$

This observation is particularly interesting for coalescing or annihilating structures, which exhibit an absorbing state in a fixed geometry with one or no arms remaining as $h \to \infty$. Such structures often occur in neutral models for competition in spatial populations [6,8], and the absorbing state corresponds to fixation of the model in one of the initial types. By standard arguments the time to fixation scales as $L^{1/\gamma} \sim r_0^{1/\gamma}$, which is much larger than $h(\infty) \sim r_0$ for large systems. For $\gamma < 1$ we not only confirm the previous (intuitive) result that there is no fixation in expanding populations in the neutral case, but also give explicitly the spatial distribution of the surviving types at large radii $r \to \infty$ as $\{X_{h(\infty)}\}$. The process X_h is much easier to simulate than Y_r, and in many cases there also exist theoretical predictions [26]. A similar approach has recently been used independently in Ref. [27] to study the heterozygosity in a radial Domany-Kinzel type model for the case $\gamma = 1/2$.

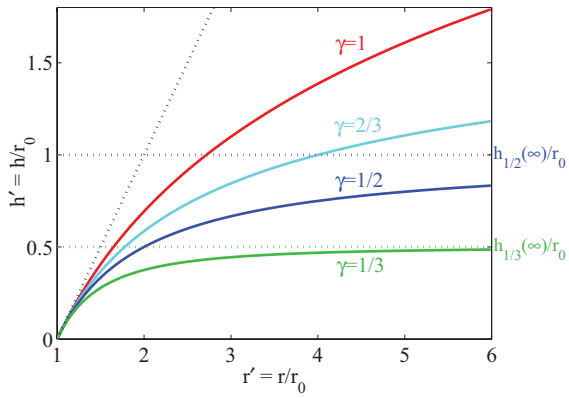

FIG. 2. (Color online) The mapping $h(r)$ between an expanding radial growth structure and the same structure on a fixed domain as given in Eq. (8) in units of r_0 [see (11)]. Due to local equivalence of the two processes, $h(r) \approx r - r_0$ for $r \approx r_0$. The different geometries affect the behavior at large r, in particular, $h(r)$ has a finite limit $h_\gamma(\infty)$ for $\gamma < 1$ (10) and diverges for $\gamma \geqslant 1$. The asymptotic behavior is indicated by dotted lines, except for $\gamma = 2/3$, which is off the figure.

In Fig. 2 we plot the mapping in convenient dimensionless variables $r' = r/r_0$ and $h' = h/r_0$, so that

$$h'(r') = \begin{cases} \frac{\gamma}{1-\gamma}(1-(1/r')^{\frac{1-\gamma}{\gamma}}), & \gamma \neq 1, \\ \log(r'), & \gamma = 1, \end{cases} \qquad (11)$$

for all $r' \geqslant 1$. For $\gamma = 1$ we recover the generic conformal map from the exterior of the unit circle to a strip, whereas for $\gamma \neq 1$ the mapping provides a natural generalization to self-affine processes. Note that for general γ, $h'(r') = \log_q(r')$ is the q logarithm with $q = 1/\gamma$ known from nonextensive statistical mechanics [28], which can therefore also be interpreted as a generalization of conformal transformations.

It is instructive to consider the mapping also for inward growing radial structures, where $r \leqslant r_0$ (i.e., $r' \leqslant 1$), which formally leads to negative heights $h < 0$, corresponding to a fixed domain structure growing downward. Observing the general relation

$$h'(1/r') = -(r')^{\frac{1-\gamma}{\gamma}} h'(r') \quad \text{for all} \quad \gamma > 0, \qquad (12)$$

all phenomena for such structures can be entirely understood by studying outward growing ones. Note that in contrast to the expanding case now all sub-ballistic structures lead to fixation since $|h'(r')| \to \infty$ as $r' \to 0$, whereas superballistic structures will have a nontrivial limit. First results on inward growing radial structures have been obtained in Ref. [29] and our approach provides a framework for a better understanding of those which is explained in detail in future work [26].

Validity and locality. The mapping is based purely on a conservation of local scale invariance of the structure. Therefore it is not surprising that the mapping can be shown to hold rigorously for processes which are fully determined by their local structure, namely, processes with independent increments such as Brownian motion and self-similar Lévy processes [30]. On the other hand, there are other self-similar processes with the same local scale invariance but more complicated temporal correlations, such as fractional Brownian motion (fBm) [31]. The correlations will influence the mapping and it does not hold in general for such processes. Using fractional stochastic calculus, one can derive a similar mapping for the particular model of fBm, which leads to a more complex expression which is numerically very close to Eq. (8). This derivation is beyond the scope of this Rapid Communication and is discussed in detail in Ref. [26].

In Fig. 3 we illustrate the validity of the mapping for self similar Lévy flights, which are defined via independent stationary increments with an α-stable jump size distribution

$$\mathbb{P}(X_{h+} - X_h = x) \sim C|x|^{-(1+\alpha)} \quad (\alpha > 0), \qquad (13)$$

as well as fBm, which can be characterized as a Gaussian process with covariances

$$\langle X_{h+\Delta h} X_h \rangle \sim (h+\Delta h)^{2\gamma} + h^{2\gamma} - (\Delta h)^{2\gamma}. \qquad (14)$$

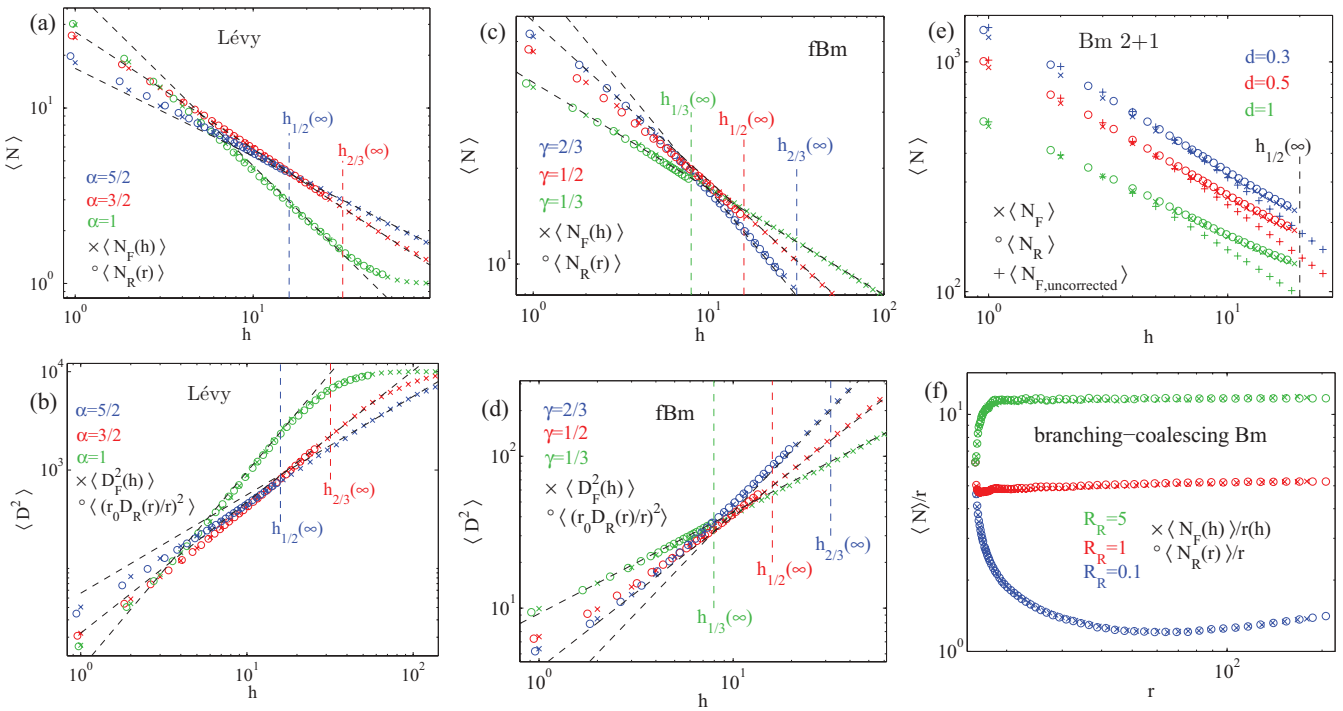

FIG. 3. (Color online) Numerical demonstration of the mapping (8) between radial geometry (∘ on all panels) and fixed domain (×): (a), (b) Number of surviving arms $\langle N \rangle$ and their root mean square distance $\langle D^2 \rangle$ (15) for Lévy flights (13) with $\gamma = \max\{1/\alpha, 1/2\}$; (c), (d) the same observables for fractional Brownian motion (14); (e) number of surviving arms for Brownian motion ($\gamma = 1/2$) with finite particle size d, + symbols indicate uncorrected, × corrected particle radii (see text); (f) radial density of arms $\langle N \rangle / r$ for branching-coalescing Brownian motion with fixed branching rate R_R (16) in the radial geometry. For (a)–(e) the horizontal axis is h or $h(r)$, with $h(\infty)$ indicated, while for (f) the horizontal axis is r or $r(h)$. The asymptotic scaling laws [black dashed lines on (a)–(d)] break down when $\langle N \rangle \approx 1$. (a)–(d) and (f) are in $1+1$ dimensions, initially 100 arms, $L = 100$ with $r_0 = L/2\pi$, while (e) is in $2+1$ dimensions with $r_0 = 20$.

Lévy flights have a local scale invariance parameter $\gamma = \max\{1/\alpha, 1/2\}$. They are superdiffusive and have noncontinuous paths for $\alpha < 2$, and scale diffusively for $\alpha > 2$ where the jump size has finite variance. fBm can be super- or subdiffusive and is not Markovian, but still the mapping (8) works very well also in that case. In Fig. 3 we compare two statistics for coalescing interaction: the average number of arms $\langle N \rangle$, and the total mean squared distance between neighboring arms, as a measure for their spatial distribution. For fixed geometry

$$D_F(h)^2 = \sum_{i=1}^{N(h)} \left(X_h^{(i+1)} - X_h^{(i)}\right)^2, \tag{15}$$

with an analogous $D_R(r)$ for radial geometry. Plotting the fixed and circular data against h and $h(r)$, respectively, we obtain a data collapse. The power-law predictions for the fixed system in Figs. 3(a)–3(d) can be derived easily by standard mean-field arguments [32,33].

A natural step to include nonlocal interactions is to introduce a particle size. For simplicity we consider isotropic shapes with diameter d, i.e., particles coagulate or annihilate already at a nonzero distance d. As long as the diameter is much smaller than the macroscopic length scale in the system, $d \ll r_0$, the corrections introduced are small. Still they can be taken into account exactly by comparing the radial system with the fixed domain one, where the particle diameter decreases as $\frac{r_0}{r(h)}d$. In Fig. 3(e) we show both cases, with and without this correction, for coalescing Brownian motions. We see that for small d the mapping still works very well even without corrections. Unlike all other numerical data presented in this Rapid Communication, this one is for an expanding sphere in $2+1$ dimensions. Finite range interactions are particularly important in higher dimensions, where coalescence or annihilation of point particles does not strictly occur, they only get arbitrarily close to each other. The mapping is independent of the dimension, as discussed below.

Another natural interaction included in growing structures is branching. This is not a purely geometric interaction but has its own characteristic rate R, which introduces a time scale in the system. For the mapped processes to have the same statistics we require that the number of branching events $\Delta_F(dh)$ in the fixed domain model during a time interval dh is the same as $\Delta_R(dr)$ for the corresponding radial system. This implies a relation between the branching rates

$$\frac{R_R}{R_F} = \frac{\Delta_R(dr)/dr}{\Delta_F(dh)/dh} = \frac{dh}{dr}, \tag{16}$$

which is $(r_0/r)^{1/\gamma}$. Thus to understand the density of branches $N_R(r)/r$ in a radially growing system with fixed branching rate R_R, one has to compare to a fixed domain system with increasing branching rate $R_F(h) = R_R\, r(h)^2/r_0^2$, where $r(h)$ is the inverse of Eq. (8). Note that this rate diverges as $r \to \infty$ or $h \to h(\infty)$. The density of branches for three different branching rates is shown in Fig. 3(f) for Brownian motions with $\gamma = 1/2$.

Generalized geometries. Our results can be directly generalized to an arbitrary time-dependent domain of size $L(t)$ with homogeneous metric. We obtain

$$h(t) = \int_0^t \left[\frac{L(0)}{L(s)}\right]^{1/\gamma} ds, \tag{17}$$

analogously to Eq. (8). For example, one can study exponentially increasing domains, which is analogous to structures with exponentially decreasing diffusivity. These have been studied in detail for single random walks [18–21] and are used in simulated annealing [34].

In $n+1$ dimensions, where n is the spatial dimensionality, our method applies directly if the scale invariance holds in all spatial directions $i = 1, \ldots, n$,

$$dX_i \sim (dh)^\gamma \quad \text{and} \quad d\tilde{Y}_i \sim (dr)^\gamma. \tag{18}$$

It is possible to have anisotropy (possible i dependence of the multiplicative factors which are not indicated), but γ should be identical in all directions. Then the mapping (17) stays exactly the same.

Summary. We have demonstrated that a large class of locally scale-invariant, directed complex structures growing in radial or general increasing geometries can be mapped to structures in fixed domains, which are simpler and for which exact results are often available. This approach provides an elegant and remarkably simple way to understand various phenomena related to time-dependent metric, such as the effect of range expansions in competitive biological growth. A particularly striking example is a full description of the limiting statistics of radial competition interfaces. Further examples and technical aspects are discussed in more detail in Ref. [26].

Acknowledgment. This work was supported by the Engineering and Physical Sciences Research Council (EPSRC), Grant No. EP/E501311/1.

[1] B. B. Mandelbrot, *The Fractal Geometry of Nature* (Freeman, New York, 1982).
[2] P. Meakin, J. Sol-Gel Sci. Technol. **15**, 97 (1999).
[3] T. A. Witten and L. M. Sander, Phys. Rev. Lett. **47**, 1400 (1981).
[4] I. Rodriguez-Iturbe and A. Rinaldo, *Fractal River Basins* (Cambridge University Press, Cambridge, UK, 1997).
[5] B. Derrida and R. Dickman, J. Phys. A: Math. Gen. **24**, L191 (1991).
[6] Y. Saito and H. Müller-Krumbhaar, Phys. Rev. Lett. **74**, 4325 (1995).
[7] R. Marchetti, A. Taloni, E. Caglioti, V. Loreto, and L. Pietronero, Phys. Rev. Lett. **109**, 065501 (2012).
[8] O. Hallatschek, P. Hersen, S. Ramanathan, and D. R. Nelson, Proc. Natl. Acad. Sci. USA **104**, 19926 (2007).
[9] K. S. Korolev, M. Avlund, O. Hallatschek, and D. R. Nelson, Rev. Mod. Phys. **82**, 1691 (2010).
[10] P. G. Saffman and G. Taylor, Proc. R. Soc. London, Ser. A **245**, 312 (1958).
[11] L. Paterson, J. Fluid Mech. **113**, 513 (1981).

[12] H. Thome, M. Rabaud, V. Hakim, and Y. Couder, Phys. Fluids A **1**, 224 (1989).
[13] O. Hallatschek and D. R. Nelson, Evolution **64**, 193 (2009).
[14] R. Lehe, O. Hallatschek, and L. Peliti, PLoS Comput. Biol. **8**, e1002447 (2012).
[15] Y. Klein, E. Efrati, and E. Sharon, Science **315**, 1116 (2007).
[16] J. Kim, J. A. Hanna, M. Byun, C. D. Santangelo, and R. C. Hayward, Science **335**, 1201 (2012).
[17] H. Lee, J. Zhang, H. Jiang, and N. X. Fang, Phys. Rev. Lett. **108**, 214304 (2012).
[18] A. C. de la Torre, A. Maltz, H. O. Mártin, P. Catuogno, and I. García-Mata, Phys. Rev. E **62**, 7748 (2000).
[19] P. L. Krapivsky and S. Redner, Am. J. Phys. **72**, 591 (2004).
[20] T. Rador, Phys. Rev. E **74**, 051105 (2006).
[21] C. A. Serino and S. Redner, J. Stat. Mech. (2010) P01006.
[22] J. Herrmann, Phys. Rev. D **82**, 024026 (2010).
[23] A. Ali and S. Grosskinsky, Adv. Complex Syst. **13**, 349 (2010).
[24] P. A. Ferrari, J. B. Martin, and L. P. R. Pimentel, Phys. Rev. E **73**, 031602 (2006).
[25] A. Ali, E. Somfai, and S. Grosskinsky, Phys. Rev. E **85**, 021923 (2012).
[26] A. Ali, E. Somfai, R. C. Ball, and S. Grosskinsky (unpublished).
[27] M. O. Lavrentovich, K. S. Korolev, and D. R. Nelson, Phys. Rev. E **87**, 012103 (2013).
[28] S. Abe and Y. Okamoto, *Nonextensive Statistical Mechanics and its Applications* (Springer, Heidelberg, 2001).
[29] N. I. Lebovka and N. V. Vygornitskii, J. Phys. A: Math. Gen. **31**, 9199 (1998).
[30] *Lévy Flights and Related Topics in Physics*, edited by M. F. Shlesinger, G. M. Zaslavsky, and U. Frisch (Springer, Berlin, 1995).
[31] F. Biagini, Y. Hu, B. Øksendal, and T. Zhang, *Stochastic Calculus for Fractional Brownian Motion and Applications* (Springer, Berlin, 2010).
[32] P. A. Alemany and D. ben Avraham, Phys. Lett. A **206**, 18 (1995).
[33] R. Munasinghe, R. Rajesh, R. Tribe, and O. Zaboronski, Commun. Math. Phys **268**, 717 (2006).
[34] S. Kirkpatrick, C. D. Gelatt, Jr., and M. P. Vecchi, Science **220**, 671 (1983).